ELSEVIER

Earth and Planetary Science Letters 185 (2001) 225–236

EPSL

www.elsevier.com/locate/epsl

India–East Antarctica conjugate margins: rift-shear tectonic setting inferred from gravity and bathymetry data

Shyam Chand [a], M. Radhakrishna [b], C. Subrahmanyam [a,*]

[a] *National Geophysical Research Institute, Uppal Road, Hyderabad 500 007, India*

[b] *Department of Marine Geology and Geophysics, School of Marine Sciences, Cochin University of Science and Technology, Cochin 682 016, India*

Received 16 May 2000; received in revised form 5 October 2000; accepted 13 November 2000

Abstract

The Eastern Continental Margin of India (ECMI) has evolved as a consequence of breakup of India from East Antarctica during the Early Cretaceous (ca. 130 Ma). The conjugate margin of ECMI in East Antarctica is represented by the margin extending from Gunneris Ridge in the west to about 95°E in the east. To understand the isostatic compensation mechanism operating beneath these conjugate margins, we have examined the cross spectral correlation between gravity and bathymetry along 21 profiles across the ECMI and 16 profiles across the conjugate East Antarctica Margin using both ship and satellite-derived gravity data. The ECMI is considered as a composite of two segments, one north of 16°N extending beyond 20°N, which is based on its rifted margin character, and the other, south of 16°N extending up to Sri Lanka, which has a transform-rift character. Similarly, the conjugate margin of East Antarctica is also considered to be a composite of two segments, west and east of the central bulge at 50–55°E. Admittance analysis and comparison with various isostatic models suggest a flexural plate model with an elastic thickness of 10–25 km for the northern segment of ECMI and its conjugate segment which is the east Enderby land Margin, comparable to results obtained from the eastern North American Margin. For the southern segment of ECMI, low elastic plate thickness of less than 5 km or a local compensation is obtained with matching results for the west Enderby land Margin. These, in turn, appear comparable to the low T_e values inferred for the Ghana transform margin of North Africa and Grand Banks Margin of eastern Canada, thereby indicating that the southern segment of ECMI and its conjugate in East Antarctica have developed as a consequence of shearing rather than rifting in the early stages of continental separation.

Keywords: continental margin; India; Antarctica; gravity anomalies; isostasy

1. Introduction

Continental margins are entities of mixed character where there is a change in physiography as well as physical properties. The morphology of the continental margin is determined by its formation mechanism (rifting vs. shearing) and processes that have subsequently operated on it. This is reflected in the gravity anomalies. Most of these margins display a positive gravity anomaly along the edge of the shelf and a negative anomaly over

* Corresponding author. Fax: +91-40-7171564; E-mail: postmast@csngri.ren.nic.in

0012-821X/01/$ – see front matter
PII: S0012-821X(00)00349-6

the slope. The amplitude of these anomalies and the distance between the positive and negative gravity anomalies are representative of the type of the margin (rifting vs. shearing) and its sedimentation pattern [1,2].

Numerous studies have addressed the relation between gravity anomalies and topography [1–4]. The effective elastic thickness (T_e) is an important parameter, which can be derived from the observations of gravity and topography as well as sediment thickness. T_e characterises the flexural response of the lithosphere subjected to topographic loading. Gravity observations in oceanic regions have been widely used to estimate T_e of the oceanic lithosphere [5–7]. It has also been applied at continental margins [1,4].

The sediments deposited in subsided areas along the continental margin act as a top load on the lithosphere. Numerous studies at rifted margins showed that they are consistent with the flexure model of isostasy [1,2,4]. Steckler and Watts [8] showed that the post-rift subsidence of margins can be attributed both to the thermal cooling of the lithosphere following initial heating up by rifting, and also due to the accumulation of sediment loads. The accommodation of these sediments and the depositional pattern of most basins suggest a flexural type of behaviour right from the start of rifting. Fowler and McKenzie [3] have compared two margins on the basis of gravity, one starved of sediments and the other, buried under sediments. This study showed that sedimentary accumulations have no effect on the flexural characteristics of the margin. Thus, the concept that the basic shape of the gravity profile is retained, even though there is deposition of sediments, forms the basis for examining the character of margins through a convolution filter [3].

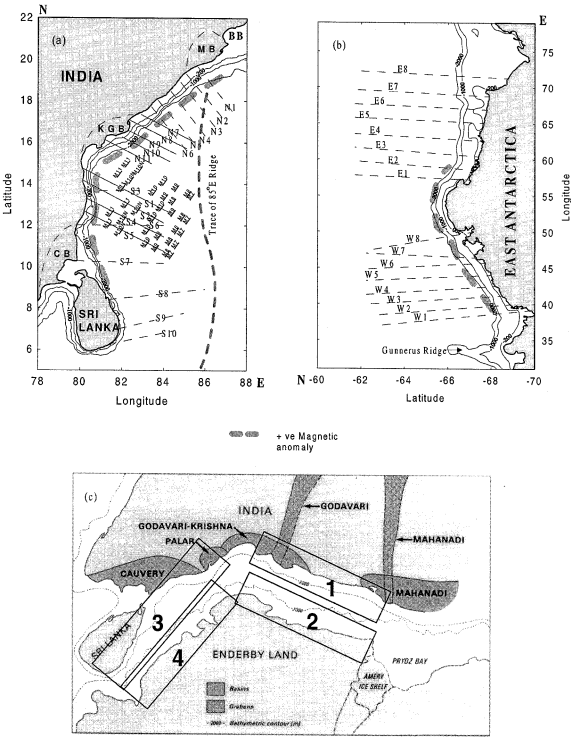

Fig. 1. (a) The ECMI showing bathymetry and locations of the profiles (S1–S10 and N1–N11) used in the present study; M1–M11 are magnetic lineations [48]; Thick grey lines are positive magnetic anomalies identified [23,24]. CB: Cauvery Basin; KGB: K–G Basin; MB: Mahanadi Basin; BB: Western margin of Bengal Basin; Trace of 85°E ridge from Subrahmanyam et al. [18]. (b) EACM showing bathymetry and locations of profiles (W1–W8 and E1–E8); Thick grey lines are positive magnetic anomalies identified by Golynsky et al. [22]. (c) India, Sri Lanka and East Antarctica in a Gondwana reassembly [49]. 1–4 indicate the conjugate segments of the ECMI and the EACM.

2. Geological setting

The Eastern Continental Margin of India (ECMI) has evolved as a consequence of its breakup from East Antarctica in Early Cretaceous [9]. This margin is characterised by major river basins like Cauvery, Krishna, Godavari, Mahanadi, Brahmaputra and Ganges, which in all cases, extend from onland to offshore and merge with the deep-sea Bengal Fan [10]. The thickness of sediments in these basins varies from 3–5 km in the onshore depressions to more than 10 km in the thick deltaic sedimentation regions of the offshore [11]. The sediments attain a maximum thickness of 22 km at the apex of the Bengal Fan in the Bangladesh offshore region [10]. Seismic studies of both the onland and offshore basins reveal NE–SW trending ridge and graben structures, which are parallel to the coast in the case of Krishna–Godavari (K–G) and Mahanadi Basins, but trend oblique to the coast in

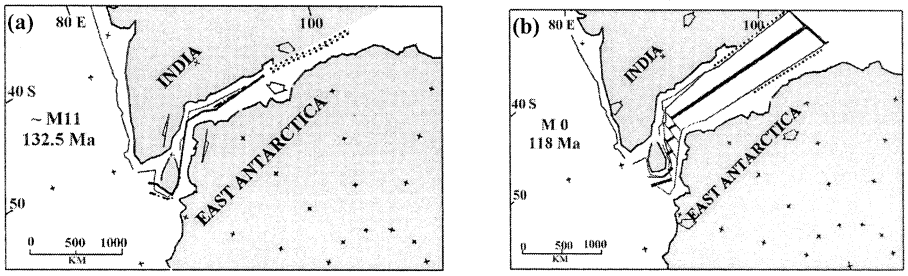

Fig. 2. Early break-up history between India and East Antarctica[9]. (a) Shearing between southern ECMI and western EACM is shown by half arrows. (b) Note the change from transform to a closely spaced transform–ridge setting.

the Cauvery Basin further south [11]. Subsidence studies in Cauvery, K–G and Bengal Basins along the ECMI, suggest that there is a progressive increase in extension rates from south to north [12–14].

Recent geophysical and geochronological inferences indicate the presence of a large igneous province underlying the Bengal Basin, related to the exposed Rajmahal Trap volcanism [15,16] with possible extension up to the Mahanadi Basin. These volcanics are dated at 118–110 Ma. Uplift of the lithosphere due to the incubation of a mantle plume head beneath the Bengal Basin and adjoining areas prior to continental rifting has earlier been suggested [17]. These factors are strong indicators for considerable uplift and stretching of the lithosphere beneath the northern segment of the ECMI, prior to the break-up of eastern India from East Antarctica. The limited extension experienced by the lithosphere beneath the Cauvery Basin [13] can probably be explained if this segment of ECMI is a transform margin or at least a margin with closely spaced ridge-transform system (as shown in Fig. 2). A recent analysis of the distribution of satellite-derived free air anomalies along the ECMI [18] and the spreading directions inferred by Powell et al. [9] support such a view. These investigations indicate that, along the southern segment of the ECMI, considerable shearing may have taken place between India and East Antarctica. The development of ridge–basin structures in the Cauvery Basin (Fig. 3) trending oblique to the coast line reflect the pull-apart nature of the basin [11], having evolved in a strike–slip setting.

The East Antarctica Margin has a similar geological history [19]. But, compared to the ECMI, the thickness of sediments along the East Antarctica Continental Margin (EACM) is less. The continental shelf around Antarctica is often characterised by a trough up to 1 km deep near the coast and an unusually deep outer shelf (400–700 m deep at the shelf edge). In some places (e.g., Prydz Bay) the water depth decreases from the coastal trough to the shelf edge, while at other places it is seen to be normal. These features were explained

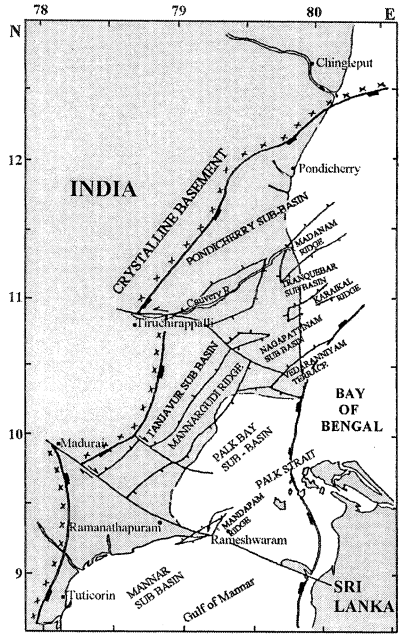

Fig. 3. Ridge–basin structures in Cauvery Basin trending oblique to the coastline modified from Sastri et al. [11].

as being due to a series of patterns of glacial erosion and sedimentation through geologic time on the shelf [20]. Several factors control the geometry of the sea floor and underlying stratigraphy of the East Antarctic Margin. These include, the load of the ice cap, the isostatic response of the lithosphere, the pattern of erosion, the pattern of sedimentation, sea-level changes, thermal and tectonic subsidence of the margin and possible compaction of the sedimentary section by sediment and episodic ice loading of the continental shelf. Unloading studies conducted along a seismic section show a variable T_e of 100 km near the coast and 30 km at the Ocean–Continent boundary [20]. Lithosphere flexure due to the load of the continental ice cap is small (<250 m) in comparison [20].

Reconstructions for the Eastern Gondwanaland [9] indicate that the present day continental margin of East Antarctica agrees well with the ECMI along 2000 m bathymetry between 35 and 95°E. Lawver et al. [21] have dated the starting of rifting of India and East Antarctica to around 127–118 Ma (M0–M5 magnetic lineations of Early Cretaceous age). Golynsky et al. [22] used airborne magnetic data to identify a prominent positive magnetic anomaly belt (Antarctic Continental Margin Magnetic Anomaly (ACMMA)), which is inferred to be due to continental crustal discontinuities that were formed during the Gondwana breakup (Fig. 1b). The ACMMA has a width of 120 km, with moderate to short wavelength anomalies of 150–600 nT, which can be taken as a counter part of the positive magnetic anomaly belt observed along the ECMI [23,24]. It can be seen on Fig. 1a,b that both these anomaly belts run along the 2000 m bathymetry contour line supporting the view about the conjugate nature of the two margins under study.

3. Data and analysis

Gravity anomaly distribution for both the margins, from satellite-derived gravity databases [25], are shown in Fig. 4. Notable features of these gravity maps are: the sharp gravity gradients along the southern segment of the ECMI, which

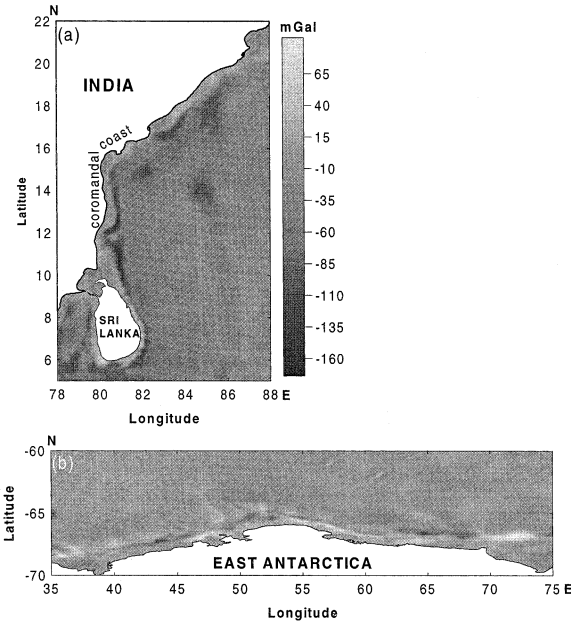

Fig. 4. Grey-scale maps of free-air gravity anomalies along the ECMI (a) and the EACM (b) from Sandwell and Smith [25].

extend up to Sri Lanka; the strong negative signature of the 85°E ridge [18] and the northwest trending gravity lineations along the EACM particularly between 45–50°E which may be related to early history of spreading between India and East Antarctica [26]. Such features, related to spreading histories, are characteristically absent along the ECMI, which may be due to their masking by thick piles of sediments present along the margin. Another notable feature along the EACM is that the negative–positive anomaly belt centred along the continental rise of the western segment of EACM differs from the usual signature of positive peak at the shelf edge followed by a negative peak over the slope.

Transfer function analysis is the most widely used method to study the compensation mechanism of loading on the lithosphere, and we have used this approach in the present study. The location of profiles used for cross-spectral correlations of gravity and bathymetry is shown in Fig. 1a,b. Blocks 1–4 in Fig. 1c indicate the rift and transform segments of the ECMI and EACM. A set of 11 gravity and bathymetry profiles almost

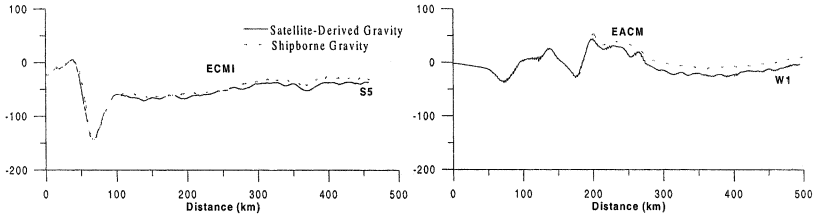

Fig. 5. Comparison of ship-borne gravity with satellite-derived gravity for profile S5 along ECMI and profile W1 along the EACM. See text for details.

perpendicular to the northern segment of ECMI (from 15 to 20°N). The five southern profiles are derived from data collected by ORV Sagar Kanya cruises [23]. Other profiles are interpolated from satellite-derived gravity [25] and ETOPO5 [27] data grids. For the southern segment of ECMI (from 6 to 15°N) we have considered 10 profiles of which four were collected during the Sagar Kanya cruise, and the rest are from the NGDC databank. For the East Antarctic region, we have considered eight profiles for each segment, all from satellite-derived gravity and ETOPO5 bathymetry. We use the Enderby Land bulge as the boundary between the two segments (Fig. 1c) corresponding to the conjugate location of the bight at 15°N along the Coromandal Coast of ECMI [9].

We have made a comparison of the satellite-derived gravity data and the ship borne gravity data to check the validity of these gridded data sets as well as the reliability of the ship data from offshore Antarctica and the ECMI (Fig. 5). The gravity data of the EACM show a datum shift, which may be attributed to the correction applied from Reference Station [28]. Nonetheless, the signatures match well showing that the satellite-derived gravity data are more reliable to be used than ship data in such areas, where Reference Stations are not available. For ECMI, the data show a good correspondence although there is a slight mismatch in the high frequency domain which may be attributed to the small disparity in location of cruise data and satellite-derived gravity data locations.

Representative samples of gravity and bathymetry profiles from both the margins are shown in Fig. 6. It can be seen that the amplitudes of the gravity anomaly are higher in the ECMI compared to the EACM, a fact which may be attributed to the wider slope of the latter (Fig. 6). The main feature observed from the bathymetry profiles is the very gentle slope along the EACM, compared to the ECMI. Because of this, the shelf edge gravity anomaly is also very small. The gravity anomalies show very low amplitudes of the order of 100 mGal as the maximum.

To examine the isostatic mechanism acting at the margins under study, we have used the cross-spectral correlations between gravity and bathymetry. The methodology involves calculating the admittance between gravity and bathymetry, and compairing it with theoretical models. Admittance analysis involves computing the ratio of the average of cross spectrum between gravity and bathymetry to average power spectrum of bathymetry [1]. This way of spectral averaging removes any spurious signals which are profile specific and thereby provides us a signal that is representative of the entire margin. The net result is the ratio of amplitude spectrum of gravity to bathymetry. For cross-spectral analysis, the length of each profile is

Table 1
Model parameters

Parameter	Value
Water density	1030 kg m^{-3}
Sediment density	2400 kg m^{-3}
Crustal density	2800 kg m^{-3}
Mantle density	3400 kg m^{-3}
Young's modulus	100 GPa
Poisson's ratio	0.25
Mean water depth	3.0 km
Gravitational constant	6.67×10^{11} $m^3kg^{-1}s^{-2}$
g	9.8 m s^{-2}

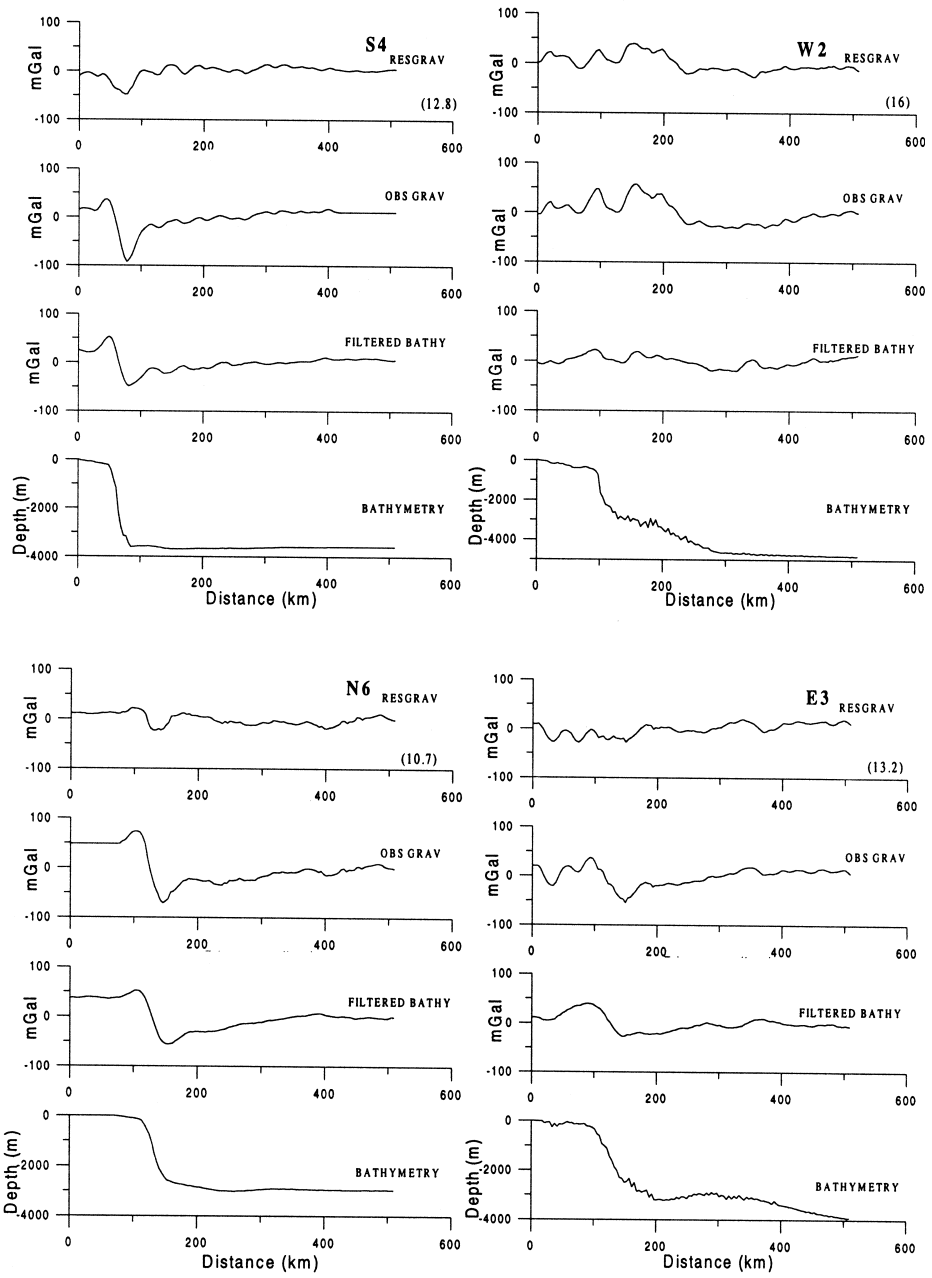

Fig. 6. Representative plots of bathymetry, filtered bathymetry (predicted gravity), observed gravity and residuals for the four segments of ECMI and EACM (shown in Fig. 1c). Numbers at the right side of the residual profile indicate RMS error.

restricted up to a 512 km length keeping the shelf edge as the tie point and starting from almost zero water depth. The profiles are linearly interpolated at 2 km intervals to a total of 256 data points. They are then mirrored, so that they are symmetric with respect to the central point. The data are then Fourier-transformed. As our profile is just half the length of the mirrored one, we took

only the alternate values corresponding to the original wave number [29] for subsequent calculations.

The methodology involved in the determination of the admittance analysis for gravity and bathymetry data has been discussed in detail by McKenzie and Bowin [5], Karner and Watts [1], among others and hence, not reproduced here. Though the Fourier Transform technique, called the periodogram method, is plagued by spectral bias and leaking resulting from the implicit windowing of finite data [30], it is found to be the most reliable method in power spectrum and cross spectrum estimation. Windowing effects can be reduced by using a large data sequence relative to the wavelengths of interest and this is why mirroring is applied on the data. However, the wavelengths of transition from high to low coherence are very long and even when the data are mirrored, the spectral properties must be computed for very large geographic areas, to be accurately resolved [31]. Flexural rigidity is assumed to be constant, as a weighted estimate of the rigidity in a geographical region. The geophysical parameters used in calculation are given in Table 1.

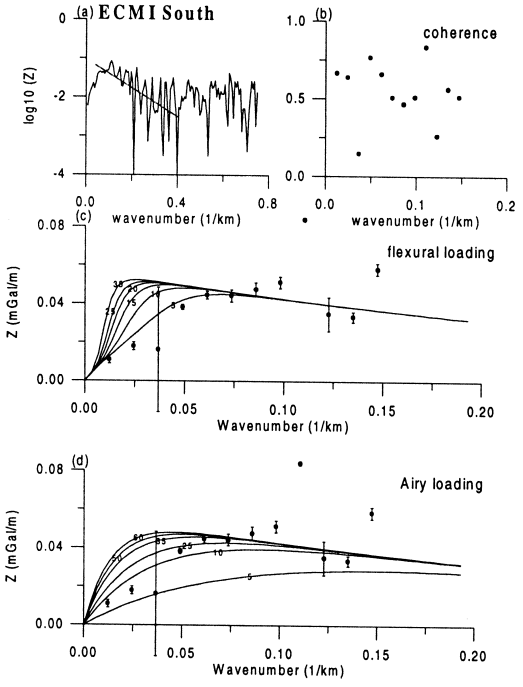

Fig. 7. Plots of (a) admittance (Z) (b) coherence (c) theoretical admittance vs. observed admittance for flexural compensation and (d) for Airy compensation, for the ECMI southern segment.

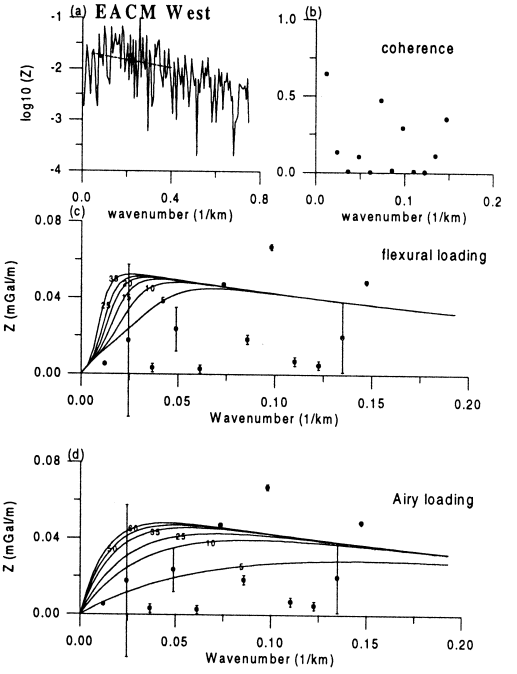

Fig. 8. As for Fig. 7, for the EACM western segment.

4. Results and discussion

Fig. 6 also shows the predicted gravity and residual along the representative profiles for the four segments under study. It can be noticed that residuals are very large for the western segment of EACM and southern segment of ECMI as compared to the other two segments. These large residuals may be reflecting the effect of the rift morphology of the basement, which is not reflected in the observed bathymetry. Such large residuals are also observed at the Grand Banks Margin [4,1]. The $\log_{10}$ admittance plot shows the general fall of the admittance values in the wave number bands of interest (0.05–0.4) as shown in Figs. 7–10. The coherence plots bring out the reliability of the admittance points. Where the coherence is low, admittance estimates were

disregarded in the analysis. A surprising feature is the low coherence for the western EACM in the representative wave number bands. This may be attributed to the peculiar type of gravity signal observed all along this segment. We have along this segment a strong negative anomaly over the slope, followed by a strong positive anomaly over the rise. This is at variance with the general gravity signature of a positive gravity over the shelf followed by a seaward negative anomaly, usually called the shelf edge anomaly. This may be attributed to the features formed at the time of rifting. The lack of any topographic features in the bathymetry also strongly points to a shallow basement dominated by basement highs and lows corresponding to these gravity features.

Results of admittance analysis for the four segments are shown in Fig. 7–10. We can match the admittance signatures of the northern segment of ECMI to eastern EACM and the southern segment to the western EACM. The T_e values obtained are given in Table 2. The comparison of the results with various isostatic models indicates a rift-type regional loading mechanism in the northern segment of ECMI as well as east Enderby Land Margin. As for the southern segment of ECMI and its conjugate, a local compensation mechanism appears probable, in view of the low T_e values ($T_e < 5$ km) obtained. Low T_e values associated with some transform margins have been reported [4,30]. The results from this study are in accordance with the results of a similar analysis of the Scotia rifted margin and the Grand Banks transform margin [4], where the admittance functions are different for the two types of margins. A major difference between the results of this work and those of Verhoef and Jackson [4] is that, in the present case, the transform margin along the ECMI seems to progress into a rifted

Table 2
Estimated T_e values for the four segments

Segment	T_e (km)
North ECMI	10–25
East EACM	10–20
South ECMI	< 5 ($T_c = 8$–15)
West EACM	< 5 ($T_c = 8$–10)

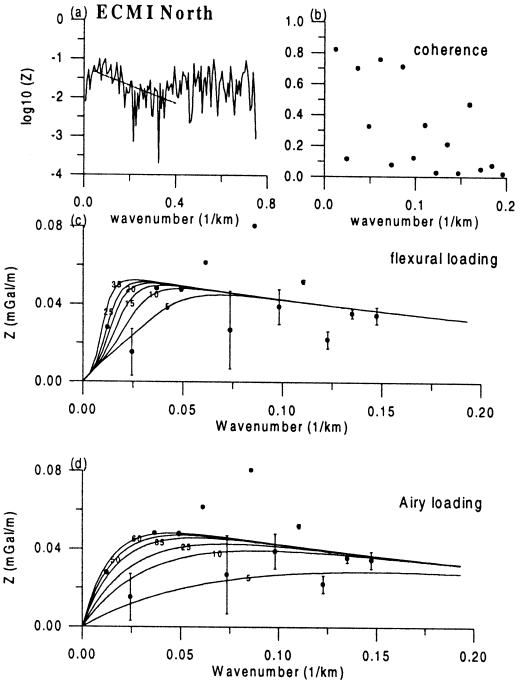

Fig. 9. As for Fig. 7, for the ECMI northern segment.

margin having moderate T_e (10–20 km) values, whereas the Grand Banks transform margin lies adjacent to a relatively weaker ($T_e = 10$ km) Scotia rifted margin.

Quite often T_e estimates are compared to brittle layer thickness derived from earthquake analysis for a variety of tectonic settings. Admittance estimates of T_e appear comparable with seismogenic thickness in case of slow spreading ridges [32,33]. In a recent study Maggi et al. [34] argued that seismogenic thickness is close to the T_e values derived for cratons. In the present case also T_e estimates seem to match well with the focal depths of earthquakes which have occurred along the ECMI [35].

Though the northernmost four profiles along the northern ECMI used in the present study have traversed across the inferred trace of the 85°E ridge [18], the results indicate that hotspot volcanism has not significantly affected the strength of the lithosphere. The high value of T_e, i.e., 10–25 km observed along northern ECMI, is comparable to 10–20 km obtained for the conjugate the eastern EACM reflecting the

rifted character of the margins which have experienced considerable stretching. On the other hand, low T_e values (<5 km) obtained for the southern segment of ECMI as well as western segment of EACM suggest local compensation and limited extension.

The T_e values for the respective segments of the conjugate margins have matching magnetic signatures as well. In the case of the northern segment of ECMI, a positive magnetic anomaly belt of considerable width is observed, which extends almost 200–250 km into the offshore, compared to the narrow bands of such anomalies seen in the southern segment of the ECMI as well as the western segment of EACM [22–24]. However, such a magnetic picture is not available for the eastern segment of EACM.

The southern segment of ECMI and its counterpart, the western EACM, appear to have experienced shearing initially at the time of continental separation followed by spreading along a closely spaced rift–transform system (see Fig. 2). The northern ECMI and the eastern EACM seem to have separated along a considerably long ridge segment, as the plate reconstruction models indicate [9]. The major difference between rifted and transform margins is that the transition from oceanic to continental crust is broader on rifted than

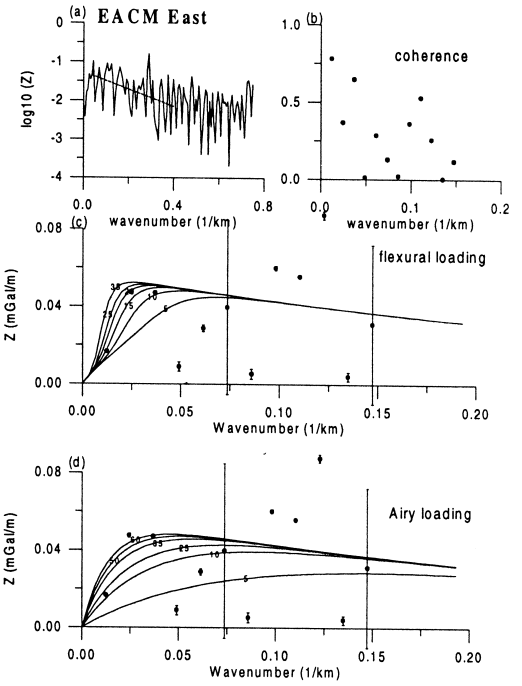

Fig. 10. As for Fig. 7, for the EACM eastern segment.

on transform margins [36]. Transform margins, in general show a low T_e value compared to rifted margins (Table 3). Seismic data across Grand Banks Margin suggests a narrow zone of shearing

Table 3
Estimates of T_e for some margins

Location	T_e (km)	Method	Type	Reference
Western Barrents Sea Margin	15	admittance	transform	[41]
Scotian Margin	5–10	admittance	rifted	[4]
Grand Banks	<1	admittance	transform	[4]
Eastern North America	10–20	admittance	rifted	[1]
Southwest Africa	5–10	admittance	rifted	[1]
Coral sea/ Lord Howe Rise	<5	admittance	rifted	[1]
Bay of Biscay Margin	8	admittance	rifted	[42]
North Sea Basin	5	forward modeling	rifted	[43]
Rockall Plateau Margin	<5	forward modeling	rifted	[3]
Exmouth Plateau Margin	5	forward modeling	transform	[3]
Ghana Margin	1.5–3.5	backstripping	transform	[39]
K–G Basin (ECMI)	30	backstripping	rifted	[14]
Western New Zealand Margin	20–28	backstripping	rifted	[44]
Baltimore canyon trough	15	backstripping	rifted	[2]
New Jersey Margin	23–30	backstripping	rifted	[45]
West Africa Margin	20	backstripping	rifted	[46]
Viking Graben	3–6	backstripping(shear)	transform	[47]

where fabric of continental crust is extremely deformed, and the faults extend through out the crust causing a weak coupling between the two regimes [37]. This supports the results from admittance studies that the Continent–Ocean transition at rifted margins is better welded than on transform margins [4]. The causes for weakening are due to the migration of rift perpendicular to the margin allowing only a brief interval when hot oceanic crust and lithosphere are adjacent to the continental crust [38]. In a margin characterised by closely spaced rift–transform system, the rift propagation is not exactly perpendicular, but oblique to the margin, which may result in some of the characters of a transform margin. The Ghana Margin provides an example of the different stages of evolution of transform margins, where a low T_e of 1.5–3.5 km is observed [39]. In comparison to other margins (Table 3), the southern segment of ECMI, as well as the western segment of EACM, compare well with the Grand Banks and Ghana Margins [4,40] where a similar rift–transform setting is inferred and the T_e values are low. On the other hand, the northern segment of ECMI, as well as the eastern segment of EACM, can be compared to the eastern North American Margin where a T_e value of 10–20 km and a normal rift mechanism are inferred [1].

The above estimates from admittance analysis are somewhat lower compared to the results obtained by the flexural backstripping method [14]. This also appears to be the case for the New Jersey Margin as compared to the Eastern North America (see Table 3). The spectral methods assume that the gravity signal results from the static deflection of a continuous thin plate (with constant elastic modulus) under loading by the surface topography or subsurface loads. Boundary forces and lithosphere discontinuities are neglected. But, in the case of a continental margin, the loads are more applied on an initial topography which has formed at the time of rifting. If sedimentation is large, depending upon the strength of the margin, the initial rift structure gets masked by the topography resulting from sediment cover. In such cases, coherence plots give an insight into the processes that has taken place viz., high coherence denoting top loading [4]. Thus the low coherence in some wave numbers indicates that the gravity is not controlled by topography and its isostatic response in this range. Features such as hidden (subsurface) loads and basement topography also significantly control gravity signatures. This is clearly seen in backstripping-based sediment unloading studies [14], where the rift architecture is brought out and accounted for. The hidden load problem was addressed by Verhoef and Jackson, [4] through an inverse admittance filter. They found that the large residuals obtained for transform margin can be explained only through subsurface loading. Any such study can only be taken through the knowledge of the size of these loads which requires seismic data which are not available in the present case.

5. Conclusions

The conjugate nature of the ECMI and EACM can be substantiated from the present admittance studies. The rheology of the margin in terms of T_e shows that the northern segment of ECMI has a value of 10–25 km compared to its counterpart, the eastern segment of EACM, which has a value of 10–20 km. In contrast, the southern segment of ECMI and western segment of EACM also show a correspondence with very low T_e values of less than 5 km. The present study establishes pure rifting between the northern segment of ECMI and the eastern segment of the EACM. On the other hand, the southern segment of ECMI seems to have separated from its conjugate, the western EACM, initially by shearing and later developing into a closely spaced transform–rift setting.

Acknowledgements

S.C. thanks the Council of Scientific and Industrial Research for the award of research fellowship to carryout this work and also Drs. N.K. Thakur, V.P. Dimri and Prof. P.S. Mohrir for useful discussions on spectral analysis. Helpful reviews from Dr. M. Kogan, Dr. G. Ramillien and an anonymous reviewer are much appreciated.

C.S. and S.C. thank the Director, National Geophysical Research Institute, Hyderabad for his permission to publish this work. *[AC]*

References

[1] G.D. Karner, A.B. Watts, On isostasy at Atlantic-type continental margins, J. Geophys. Res. 87 (1982) 2923–2948.

[2] A.B. Watts, Gravity anomalies, crustal structure and flexure of the lithosphere at the Baltimore Canyon Trough, Earth Planet. Sci. Lett. 89 (1988) 221–238.

[3] S. Fowler, D. McKenzie, Gravity studies of the Rockall and Exmouth Plateaux using SEASAT altimetry, Bas. Res. 2 (1989) 27–34.

[4] J. Verhoef, H.R. Jackson, Admittance signatures of rifted and transform margins: examples from eastern Canada, Geophys. J. Int. 105 (1991) 229–239.

[5] D. McKenzie, C.O. Bowin, The relationship between bathymetry and gravity in the Atlantic Ocean, J. Geophys. Res. 81 (1976) 1903–1915.

[6] A.B. Watts, An analysis of isostasy in the World Oceans, 1. Hawaiian–Emperor Seamount chain, J. Geophys. Res. 83 (1978) 5989–6004.

[7] A.B. Watts, G.D. Karner, M.S. Steckler, Lithosphere flexure and the evolution of sedimentary basins, Phil. Trans. R. Soc. 305 (1982) 249–282.

[8] M.S. Steckler, A.B. Watts, Subsidence of the Atlantic-type continental margin off New York, Earth Planet. Sci. Lett. 41 (1978) 1–13.

[9] C.McA. Powell, S.R. Roots, J.J. Veevers, Pre-breakup continental extension in East Gondwanaland and the early opening of the eastern Indian Ocean, Tectonophysics 155 (1988) 261–283.

[10] J.R. Curray, Possible green schist metamorphism at the base of a 22 km sedimentary section in Bay of Bengal, Geology 19 (1991) 1097–1100.

[11] V.V. Sastri, R.N. Sinha, G. Singh, K.V.S. Murti, Stratigraphy and tectonics of sedimentary basins on east coast of peninsular India, Am. Assoc. Pet. Geol. Bull. 57 (1973) 655–678.

[12] M.V.N. Chari, B. Banerjee, Subsidence history of Bengal Basin, in: Proc. Second Seminar on Petroliferous Basins of India, Indian petroleum publishers, Dehra Dun 1 (1993) 47–59.

[13] M.V.N. Chari, J.N. Sahu, B. Banerjee, P.L. Zutshi, K. Chandra, Evolution of the Cauvery Basin, India from subsidence modeling, Mar. Pet. Geol. 12 (1995) 667–675.

[14] M. Radhakrishna, S. Chand, C. Subrahmanyam, Gravity anomalies, sediment loading and lithospheric flexure associated with Krishna–Godavari Basin, Eastern Continental Margin of India, Earth Planet. Sci. Lett. 175 (2000) 223–232.

[15] A.B. Watts, K.G. Cox, The Deccan traps: an interpretation in terms of progressive lithospheric flexure in response to a migrating load, Earth. Planet. Sci. Lett. 93 (1989) 85–97.

[16] M. Mukhopadhyay, M.R. Krishna, Geophysical evidences for Crustal Transition under the Eastern Continental Margin of India, Geol. Surv. Ind. Spl. Pub. No. 29 (1992) 87–103.

[17] R. Kent, Lithospheric uplift in Eastern Gondwana: Evidence for a long-lived mantle plume system, Geology 19 (1991) 19–23.

[18] C. Subrahmanyam, N.K. Thakur, T. Gangadhara Rao, Tectonics of the Bay of Bengal: new insights from satellite-gravity and ship-borne geophysical data, Earth Planet. Sci. Lett. 171 (1999) 237–251.

[19] D. Johnson, Mc.A.C. Powell, J.J. Veevers, Spreading history of the eastern Indian Ocean and Greater India's northward flight from Antarctica and Australia, Geol. Soc. Am. Bull. 87 (1976) 1560–1566.

[20] U.S. ten Brink, A.K. Cooper, Modeling the bathymetry of the Antarctic continental shelf, in: Y. Yoshida, K. Kaminuma, K. Shiraishi (Eds.), Recent progress in Antarctic Earth science, Terra Scientific publishing company, Tokyo (1992) 763–771.

[21] L.A. Lawver, J.Y. Royer, D.T. Sandwell, C.R. Scotese, Crustal development: Gondwana break-up, in: M.R.A. Thomson, J.A. Crame, J.W. Thomson (Eds.), Geological Evolution of Antarctica, Cambridge Univ. Press, Cambridge (1991) 533–539.

[22] A.V. Golynsky, V.N. Maolov, Y. Nogi, K. Shibuya, C. Tarlowsky, P. Wellman, Magnetic anomalies of Precambrian terranes of the East Antarctic shield coastal region (20°E 50°E), Proc. NIPR Symp. Antarct. Geosci. 9 (1996) 24–39.

[23] K.S.R. Murthy, T.C.S. Rao, A.S. Subrahmanyam, M.M. Malleswara Rao, S. Lakshminarayana, Structural lineaments from the magnetic anomaly maps of the eastern continental margin of India (ECMI) and NW Bengal Fan, Mar. Geol. 114 (1993) 171–183.

[24] T.C.S. Rao, V. Bhaskara Rao, Some structural features of the Bay of Bengal, Tectonophysics 124 (1986) 141–153.

[25] D.T. Sandwell, W.H.F. Smith, Marine gravity anomaly from Geosat and ERS-1 satellite altimetry, J. Geophys. Res. 102 (1997) 10039–10054.

[26] D.T. Sandwell, D.C. McAdoo, Marine gravity of the Southern Ocean and Antarctic margin from GEOSAT: tectonic complications, J. Geophys. Res. 93 (1988) 10389–10396.

[27] Earth Topography (ETOPO5), Relief map of the earth's surface, EOS, Trans. Am. Geophys. Union 67 (1986) 121.

[28] K.M. Marks, Resolution of the Scripps/NOAA marine gravity field from satellite altimetry, Geophys. Res. Lett. 23 (1996) 2069–2072.

[29] M. Diament, Influence of method of data analysis on admittance computation, Ann. Geophys. 3 (1985) 785–792.

[30] S.M. Kay, Modern Spectral Estimation, Prentice-Hall, Englewood Cliffs, NJ, 1988.

[31] A.R. Lowry, R.B. Smith, Flexural rigidity of the Basin

and range-Colorado Plateau–Rocky Mountain transition from coherence analysis of gravity and topography, J. Geophys. Res. 99 (1994) 20123–20140.
[32] N.C. Mitchell, Distributed extension at the Indian Ocean triple junction, J. Geophys. Res. 96 (1991) 8019–8043.
[33] B. Ashalatha, C. Subrahmanyam, R.N. Singh, Carlsberg Ridge, northern Indian Ocean: gravity and isostasy, Geophys. J. Int. 119 (1994) 69–77.
[34] A. Maggi, J.A. Jackson, D. McKenzie, K. Priestley, Earthquake focal depths, effective elastic thickness, and the strength of the continental lithosphere, Geology 28 (2000) 495–498.
[35] A.S. Subrahmanyam, K. Venkateswarlu, K.S.R. Murthy, M.M. MallesaraRao, K. Mohana Rao, Y.S.N. Raju, Neotectonism – An offshore evidence from eastern continental shelf off Visakhapatnam, Curr. Sci. 76 (1999) 1251–1255.
[36] R.A. Scrutton, Crustal structure and development of sheared passive continental margins, in: R.A. Scrutton (Ed.), Dynamics of Passive Margins, Geodynamic series, vol. 6, Am. Geophy. Union, Washington, DC (1982) 133–140.
[37] C.E. Keen, W.A. Kay, W.R. Roest, Crustal anatomy of a transform continental margin, Tectonophysics 173 (1990) 527–544.
[38] I. Reid, Effects of lithospheric flow on the formation and evolution of a transform margin, Earth. Planet. Sci. Lett. 95 (1989) 38–52.
[39] P.D. Clift, J.M. Lorenzo, Flexural unloading and uplift along the Cote d'Ivoire–Ghana transform Margin, J. Geophys. Res. 104 (1999) 25257–25274.
[40] A.B. Watts, J. Stewart, Gravity anomalies and segmentation of the continental margin offshore West Africa, Earth. Planet. Sci. Lett. 156 (1998) 239–252.
[41] E. Burov, C. Jaupart, J.C. Marechal, Large-scale crustal heterogeneities and lithosphere strength in cratons, Earth. Planet. Sci. Lett. 164 (1998) 205–219.
[42] M. Diament, J.C. Sibuet, A. Hadaoui, Isostasy of the Northern Bay of Biscay continental margin, Geol. J. R. Astron. Soc. 86 (1986) 893–907.
[43] P.J. Barton, R.J. Wood, Tectonic evolution of the North Sea Basin: crustal stretching and subsidence, Geol. J. R. Astron. Soc. 79 (1984) 987–1022.
[44] W.E. Holt, T.A. Stern, Sediment loading on the Western platform of the New Zealand Continent: implications for the strength of a continental margin, Earth Planet. Sci. Lett. 107 (1991) 523–538.
[45] M.S. Steckler, S.M. Gregory, K.G. Miller, N.C. Blick, Recoonstruction of Tertiary progradation and cliniform development on the New Jersey passive margin by 2D backstripping, Mar. Geol. 154 (1999) 399–420.
[46] A.J. Breivik, J. Verhoef, J.I. Faleide, Effect of thermal contrasts on gravity modeling at passive margins: Results from the western Barents Sea, J. Geophys. Res. 104 (1999) 15293–15311.
[47] N.J. Kusznir, G. Marsden, S.J. Egan, A flexural cantilever simple-shear/pure shear model of continental lithosphere extension: applications to the Jeanne d'Arc – Basin, Grand Banks and Viking Graben, North Sea, in: A.M. Roberts, G. Yielding, B. Freeman (Eds.), The Geometry of Nornal faults, Geol. Soc. Spec. Publ. 56 (1991) 41–60.
[48] M.V. Ramana, V. Subrahmanyam, A.K. Chaubey, T. Ramprasad, K.V.L.N.S. Sarma, K.S. Krishna, M. Desa, G.P.S. Murty, Structure and origin of the 85°E ridge, J. Geophys. Res. 102 (1997) 17995–18012.
[49] A. Cooper, H. Stagg, E. Geist, Seismic stratigraphy and structure of Prydz Bay, Antarctica: implications from Leg 119 drilling, Proc. ODP 119 (1991) 5–25.